# New phase for one-component hard spheres

Guang-Wen Wu and Richard J. Sadus[a)]
*Centre for Molecular Simulation, Swinburne University of Technology, P.O. Box 218, Hawthorn, Victoria 3122, Australia*

(Received 14 March 2003; accepted 18 March 2004)

A completely new phase for one-component hard spheres is reported in an unexpected region of the phase diagram. The new phase is observed at compressibility factors intermediate between the solid and the metastable branches. It can be obtained from either Monte Carlo simulations alone or a combination of Monte Carlo and molecular dynamics calculations. An analysis of the intermediate scattering function data shows that the new phase is in a stable equilibrium. Radial distribution function data, configurational snapshots, bond order parameters, and translational order parameters obtained from molecular simulations indicate that the new phase is significantly different from the isotropic liquid, metastable, or crystalline phases traditionally observed in hard sphere systems. This result significantly changes our previous understanding of the behavior of hard spheres. © *2004 American Institute of Physics.* [DOI: 10.1063/1.1739212]

## I. INTRODUCTION

The simplest and one of the most widely used models in molecular simulation is that of the hard sphere.[1–7] The existence of a liquid–solid transition is very well documented[3–5] but the ability of one-component hard spheres to display a glass transition is uncertain.[7–10] Glasses[11–14] are typically formed by supercooling (quenching) suitable viscous liquids. The result is a distinctive form of matter that is neither a liquid nor a conventional solid. This intermediate nature of glass makes it of considerable scientific interest, particularly for the development of theories of phase transformations. Glass formation can be studied via molecular simulation[15] techniques such as Monte Carlo simulation or molecular dynamics. If a glass transition exists, it is generally expected to occur along the metastable[16,17] extension of the fluid branch of the hard sphere phase diagram. In this work, we report molecular simulation data for one-component hard spheres, which show the formation of a new phase in an unexpected region of the phase diagram. We demonstrate that this new phase is stable and that it is different from conventional isotropic liquid, metastable, and crystalline phases.

## II. SIMULATION DETAILS

Monte Carlo simulations were performed in the canonical ensemble. Hard spheres are athermal and as such, their properties are independent of temperature ($T$). This means the canonical ensemble becomes an $NV$ ensemble in which the number of particles ($N$) and volume ($V$) are the external control parameters. The system was typically composed of 500 or 1372 identical hard spheres of diameter $\sigma$. However, we also studied systems as large as 32 000 to check for finite size effects. The hard sphere intermolecular potential ($u(r)$) at different separations ($r$) has either a value of 0 ($r>\sigma$) or $\infty$ ($r\leqslant\sigma$) depending on whether or not the spheres overlap. At each specified packing fraction ($\eta=\pi N\sigma^3/6\,\mathrm{V}$), the compressibility factor ($Z=pV/NkT$, where $p$ is the pressure and $k$ is Boltzmann's constant) was obtained by using the formula for hard spheroids[18,19] that count particle contacts. Conventional periodic boundary conditions were used and the maximum displacement of translation was adjusted to have a 50% acceptance rate. The simulations were performed in cycles with each cycle representing 500 or 1372 attempted displacements. Typically, at least 200 000 cycles were used for equilibration and, at least, a further 200 000 cycles postequilibration were performed to obtain ensemble averages of both the compressibility factor and radial distribution function ($g(r^*), r^*=r/\sigma$). Therefore, the absolute statistical uncertainty of data reported here is very low, typically $\leqslant$0.1%.

## III. RESULTS AND DISCUSSION

### A. Location of the new phase

Figure 1 compares the compressibility factor as a function of packing fraction obtained from different simulations (as detailed below). At low packing fractions ($\eta<0.494$), the system is an isotropic fluid. However, after the freezing point ($\eta_f=0.494$), three distinct alternative branches start to emerge depending on the simulation strategy. The isotropic fluid can be ''supercooled'' beyond its freezing point to generate a metastable extension (phenomenon I), which continues until a random close packing (rcp) limit[20] is reached ($\eta_{\mathrm{rcp}}=0.64$). It is along this metastable branch that efforts in the literature to find a glass transition have been *exclusively* focused. A solid-phase curve appears at moderate values of packing fraction and compressibility factor, rapidly rising to higher values until the face centred cubic (fcc) hard sphere packing fraction limit ($\eta_{\mathrm{fcc}}=0.7405$) is reached (phenomenon II). This is the conventional description of the phase diagram of a hard sphere system. The fluid–solid transition is examined in greater detail in the inset diagram of Fig. 1. By drawing a tie line from the accepted freezing packing fraction ($\eta_f=0.494$), we obtain the generally accepted value

a)Author to whom correspondence should be addressed. Electronic mail: rsadus@swin.edu.au

 

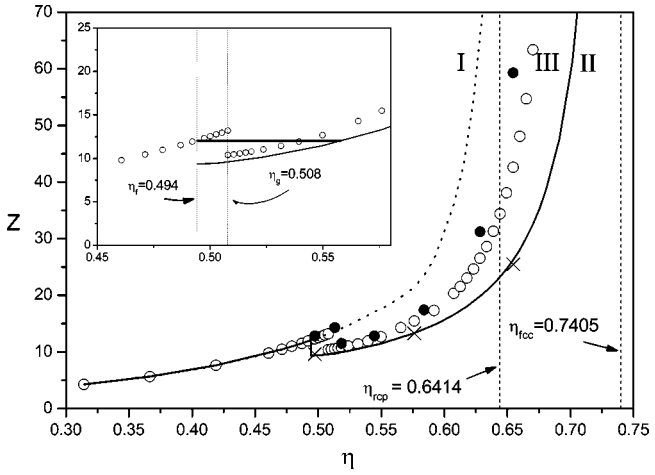


FIG. 1. The compressibility factor as a function of packing fraction obtained from different Monte Carlo and molecular dynamics simulations. At low $\eta$, an isotropic fluid is observed. However, above the freezing point ($\eta > 0.494$), three alternative phenomena are possible. Phenomenon I (-----) (Monte Carlo data), represents a metastable extension of the isotropic fluid curve, whereas phenomenon II (—) (Monte Carlo data) represents a solid phase. In the literature, a glass phase is expected along I. However, we observe a distinct new phase (phenomenon III) at $\eta \geqslant 0.508$ (○) (Monte Carlo data) at compressibility factors between the metastable fluid phase and the solid phase. In all three cases the average statistical uncertainty in the simulation data is ≤0.1%. The points marked (×) represent molecular dynamics data obtained starting from a fcc lattice configuration, whereas (●) denotes molecular dynamics data obtained using starting configurations on the metastable curve. The inset shows the transition region in greater detail. In the inset the horizontal line is a tie line between the coexisting phases.

of the melting point packing fraction ($\eta_m = 0.558$). We emphasize that this conventional fluid–solid transition could only be obtained if the simulations were initiated from a fcc lattice.

In addition to these well-known possibilities, we have observed another *new* alternative. After ''supercooling'' beyond the freezing point, instead of obtaining a metastable extension of the isotropic fluid curve, a transition is observed resulting in a new phase curve at compressibility factors *between* the solid-phase curve (phenomenon II) and the metastable curve (phenomenon I).

The nature of the simulation determines whether phenomena I, II, or III is observed. Conventionally, molecular simulations at different densities are commenced by positioning particles on a fcc lattice and allowing the lattice to ''melt'' as a result of particle displacements. If this approach is used, *only* phenomenon II is observed. The metastable extension[20] of the isotropic fluid curve associated with phenomenon I is obtained by using the final configuration of the previous density as the new initial starting point and reequilibrating the system to eliminate any overlaps caused by the increase in density. By progressively adopting this procedure, we have been able to trace the metastable curve to $\eta = 0.6414$. This is consistent with literature estimates[16] of the rcp limit. We found that if the freezing point configuration was used as the initial configuration and the density increment for the simulations was $\Delta\rho \leqslant 0.0005$, the compressibility factor obtained for the new configuration was in between that of the solid phase and the metastable curve. Closer examination (detailed below) indicated the formation of a new phase (phenomenon III). By adopting this procedure in the vicinity of the freezing point, we have identified that the transition to the new phase occurs at $\eta_g = 0.508$, which is between the conventional[16] freezing ($\eta_f = 0.494$) and melting points ($\eta_m = 0.558$) associated with the solid–fluid transition of phenomenon II. We have been able to trace the new phase curve from $\eta_g = 0.508$ to a maximum packing fraction of $\eta = 0.686$.

The phenomenon III curve was traced from low to high packing fractions by progressively incrementing the packing fraction by less than 0.03. The previous configuration was used as the initial starting configuration for each new value of packing fraction. The only way to obtain packing fractions above that of the rcp is to quench the system step by step. The step size must be sufficiently small to avoid jams and to allow the easy removal of any overlaps caused by the compression. Before every simulation at a higher packing fraction, it is important that the previous simulation had been equilibrated long enough to remove any jamming structure that will result in failure of the simulation at very high packing fractions. We note that some molecular dynamics results[21] also indicate the existence of a third curve. In contrast to our results, this appears to be a deviation from the metastable branch, which commences at much higher density ($\rho > 1.15$) and compressibility factor ($Z > 40$).

The abrupt discontinuity between the isotropic fluid curve and the new phase (Fig. 1, phenomenon III) strongly indicates that the changeover between fluid and the new phase occurs via a phase transition. In contrast, recent[22] Monte Carlo simulations for two-dimensional polydisperse hard disks display a continuous evolution between fluid and glass structures without a thermodynamic phase transition.

Although most of the simulations reported in this work are for a relatively small system size of either 500 or 1372 particles, we have also performed Monte Carlo simulations for systems with particles ranging from 1372 to 32 000 hard spheres to test whether or not results are system size dependent. Phenomenon III was observed in all cases, irrespective of the number of hard spheres used.

### B. Equilibrium stability of the new phase

To determine whether or not the new phase is in stable equilibrium we calculated the self intermediate scattering function $F(q,t)$ as defined by Hansen and McDonald[23] at the $q$ value at which the dynamic structure factor ($S(q)$) has its maximum. The analysis was similar to that performed for glasses elsewhere.[24,25] At equilibrium, $F(q,t)$ must approach zero and it should be a function of $t-t'$. In Fig. 2, $F(q,t)$ is shown as a function of $t-t'$ for three packing fractions $\eta = 0.524$, 0.634, and 0.670 along curve III. For each value of $\eta$, the analysis was conducted using ''time'' intervals of 25, 50, 100, and 200 Monte Carlo cycles. It is apparent that, irrespective of the step size or packing faction, $F(q,t)$ goes to zero. This indicates that phenomenon III has reached a stable equilibrium.

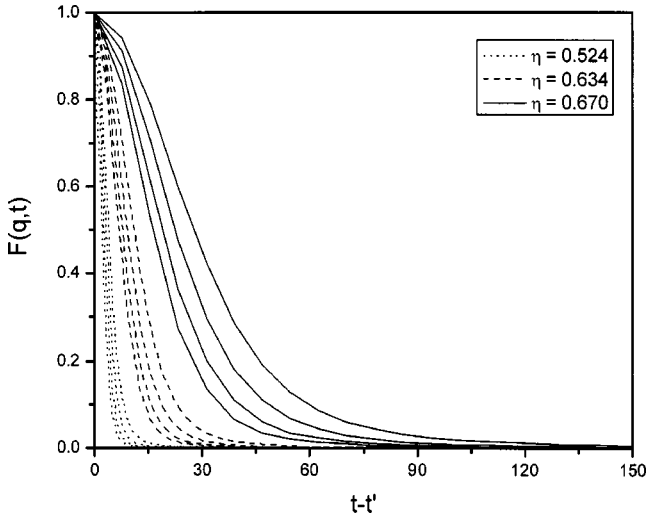


FIG. 2. The self intermediate scaterring function for phenomenon III at different packing fractions and time intervals. For each packing fraction, data for four different Monte Carlo "time" intervals are illustrated. At each packing fraction, starting from the outer most curve, results are shown for intervals of 25, 50, 100, and 200 cycles, respectively.

### C. Structural properties of the new phase

To examine the structural difference among phenomena I, II, and III, we calculated the radial distribution function at a value of $\eta=0.524$ (Fig. 3). This packing fraction was chosen because it is only slightly beyond the freezing point and it is common to phenomena I, II, and III. Peaks in $g(r^*)$ indicate the probability of locating a neighboring sphere at a given separation. The absence of peaks with increasing separation is generally characteristic of a fluid structure. The $g(r^*)$ behavior for the metastable phase largely conforms to the expected fluid pattern, although there is a small hump in the second peak indicating more order than a purely isotropic fluid. In contrast, the highly ordered nature of a solid is evident by several well-defined peaks at regular intervals. The profile of the radial distribution function of the new phase is inbetween these extremes, indicating the onset of considerable order. Like the solid phase, the new phase shows the development of a shoulder peak after the first main peak, and more clearly defined peaks in the vicinity of $r^*=2$ and 3. The height of the first peak in the $g(r^*)$ profile for the metastable curve $(g(r^*)=6.11)$ is considerably greater than for either the new phase $(g(r^*)=4.62)$ or the solid $(g(r^*)=4.26)$. This progressive reduction in the height of the first peak is also consistent with the phase assigned to the different phenomena.

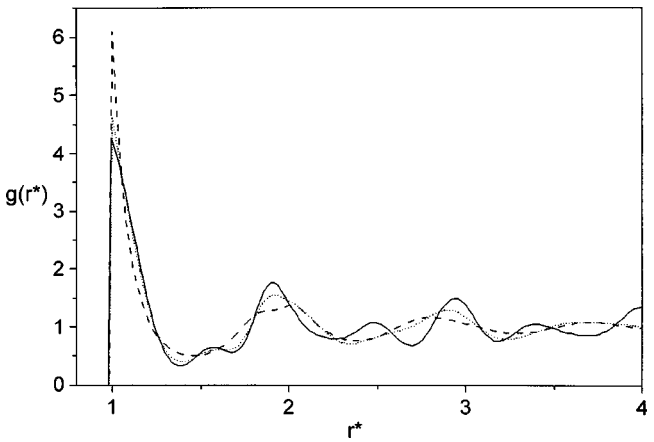


FIG. 3. Comparison of the radial distribution functions for phenomena I (— — —), II (——), and III (····) at a common packing fraction $\eta=0.524$. The different $g(r^*)$ profiles confirm the structure of I is fluid-like, II is solid-like, and III is different from these conventional phases.

In addition to the quantitative evidence provided by the radial distribution functions, configurational snapshots provide strong qualitative evidence of the structural difference between the phases. In Fig. 4, two-dimensional snapshots in the $x-y$ plane of the three-dimensional configurations of these states are illustrated. The hard spheres of the metastable phase [Fig. 4(a)] are largely randomly distributed, whereas the hard spheres in the solid [Fig. 4(c)] are concentrated around fcc lattice sites. In contrast, the hard spheres in the new phase [Fig. 4(b)] are arranged with much greater order than in the conventional metastable phase. A distinct pattern is apparent in the snapshot but the clustering around fcc lattice sites that is observed in the solid is absent.

Values of the order parameter $(S)$[26] can also be used to a quantifiable measure of the order of different phases. Isotropic phases have values of $S$ close to 0 whereas the limiting value of 1 indicates a fully crystalline phase. The variation of the order parameter as a function of packing fraction for phenomena I, II, and III is illustrated in Fig. 5. The values of $S$ for phenomenon I are low, which is consistent with an isotropic fluid and its metastable extension beyond the freezing point. The values of $S$ for phenomenon II are much larger and approach unity at high packing fractions. This is consistent with the order expected in a crystalline solid. In contrast, values of $S$ for phenomenon III are much lower than those observed for phenomenon II and they are considerably higher than the case for phenomenon I. The values of $S$ for phenomenon III are in good agreement with the range of values assigned to glasses by Truskett *et al.*[27]

To further analyze the structure of the new phase, the bond-order parameter method[28] was used. The bond-order parameter method involves determining the fraction of particles with a common number of connections or nearest neighbors. The method assumes a predetermined lattice structure. If the simulated configuration is a perfect lattice, all particles have the same number of nearest neighbors as determined by the lattice geometry. A deviation from this reference value is an indication of both the degree of crystallinity and the validity of the chosen lattice structure. We applied the bond-order method to analyze the new phase for both body centered cubic (bcc) and fcc lattices. Figures 6(a) and 6(b) illustrate the fraction of hard spheres as a function of nearest neighbors for curves I, II, and III. In the limiting case of a pure bcc or fcc structure, 100% of all hard spheres should have 8 and 12 nearest neighbors, respectively.

Figures 6(a) and 6(b) clearly illustrate the structural difference among phenomena I, II, and III. It is apparent from Fig. 6(b) that none of the phases corresponds to a bcc lattice. In contrast, Fig. 6(a) clearly shows that the solid phase (phenomenon II), forms a fcc lattice because all the hard spheres have 12 nearest neighbors. The analysis also highlights a

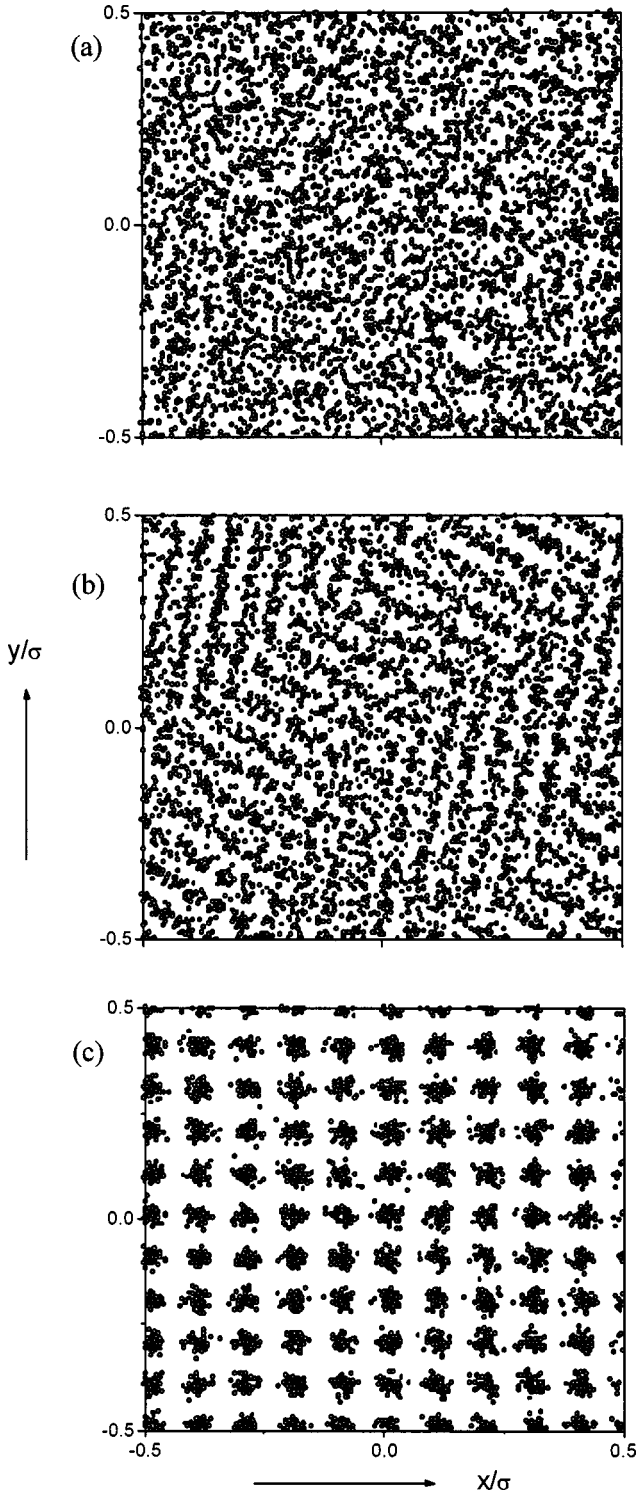


FIG. 4. Two-dimensional snapshots in the $x-y$ plane of the three-dimensional postequilibrium configuration of the: (a) metastable fluid (phenomenon I), (b) new phase (phenomenon III), and (c) solid (phenomenon II) at a common packing fraction of $\eta=0.524$. The snapshots were obtained by combing ten different postequilibration configurations separated by 5000 cycles. The different degree of ordering between the phases is clearly apparent with a distinct ordered pattern apparent for phenomenon III.

clear distinction between the isotropic fluid and its metastable extension compared with either phenomena II or III. Examining Fig. 6(a) indicates that only a tiny fraction of hard spheres in the isotropic fluid have more than four neighbors, whereas neighbors ranging from 1 to 12 are almost equally possible for the metastable extension of the isotropic fluid curve. The isotropic phase bond-order parameter behavior is consistent with that reported for a Lennard-Jones fluid.[28] The considerable degree of order in the structure of phenomenon III observed in the radial distribution function, configurational snapshots, and structure factor data is also evident in Fig. 6(a). Approximately 60% of hard spheres

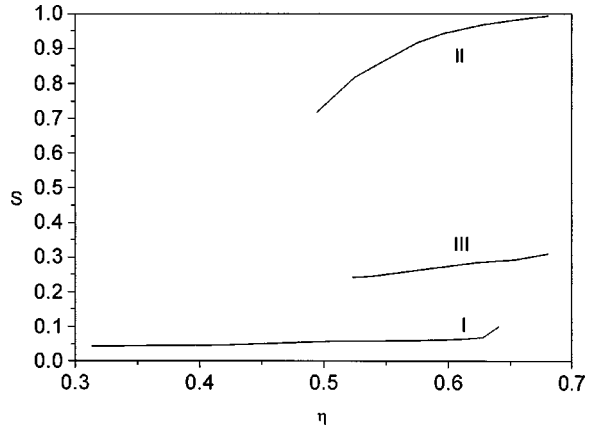


FIG. 5. Variation of the order parameter as a function of packing fraction for phenomena for phenomena I, II, and III.

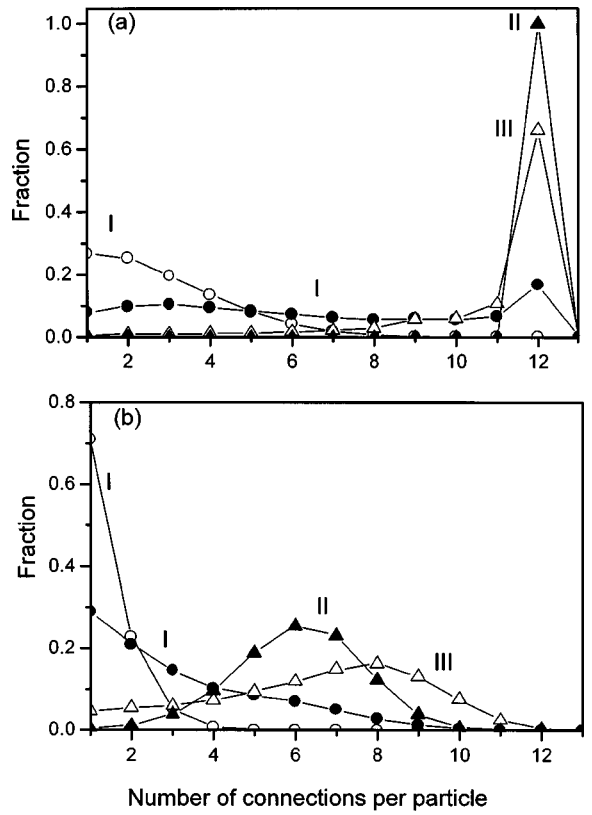


FIG. 6. Distributions of the number of connections per particle for thermally equilibrated system of 32 000 hard spheres assuming: (a) fcc and (b) bcc coordination. Results are given for phenomena I (○) $\rho=0.9$ (isotropic); (●) $\rho=1.1$ (metastable), II (▲) $\rho=1.22$, and III (△) $\rho=1.22$. The distributions are the averaged values obtained for 50 configurations. The lines are simply intended to guide the eye and should not be interpreted that fractional connections are possible.

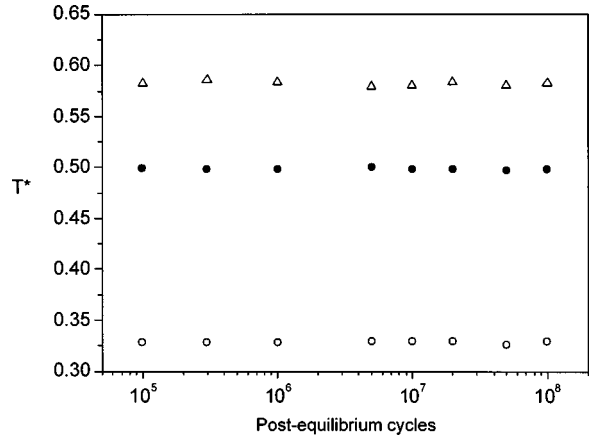


FIG. 7. Translational order parameters as a function of the number of postequilibrium configurations at different packing fractions along the phenomenon III curve. Results are shown for $\eta=0.524$ (○), 0.634 (●), and 0.670 (△).

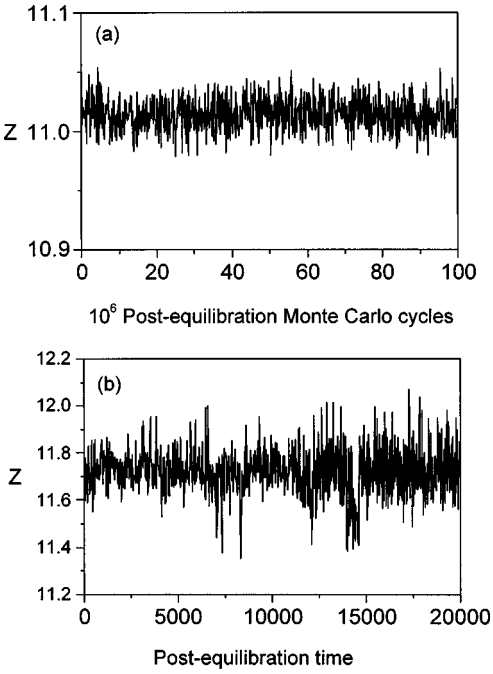


FIG. 8. Variation of the compressibility factor of phenomenon III at $\eta=0.524$ as a function of: (a) postequilibration Monte Carlo cycles and (b) postequilibration reduced time ($t^*=t(\sigma/\sqrt{m/kT})$) from molecular dynamics.

have 12 nearest neighbors. Clearly, the structure of phenomenon III does not conform to either a metastable phase or a conventional solid.

The bond-parameter method requires us to assume a predetermined crystal geometry. Truskett *et al.*[27] defined a translational order parameter ($T^*$) to provide a crystal-independent measure or order. We used the same procedure for calculating $T^*$ as reported by Truskett *et al.*,[27] which involves determining the density–density correlations by integrating over the absolute value of the total correlation function. We used their procedure to obtain values of the translational order parameter[27] at different densities and postequilibrium configurations (Fig. 7). The values of $T^*$ shown in Fig. 7 are consistent with the values attributed to glasses by Truskett *et al.*[27] The analysis is also further evidence that the phase is in equilibrium. If the phase had not reached equilibrium and was not homogeneous, we would expect $T^*$ to be sensitive to a number of postequilibrium configurations. Instead, Fig. 7 shows that for a given packing fraction, $T^*$ is remarkably constant even up to 100 million postequilibrium cycles.

### D. Ergodicity

We have performed tests to check that the new phase is genuine. The process of quenching has been repeated at several different starting packing fractions within the isotropic fluid region using different intervals of packing fraction. Phenomenon III was reproduced in these different simulations, which indicates that it is not dependent on the initial configurations. To test that the simulations have been properly equilibrated, we monitored configurations for millions of Monte Carlo cycles beyond the equilibration point. Figure 8(a) shows the variation of the compressibility factor for the new phase at $\eta=0.524$ for up to 100 million postequilibration Monte Carlo cycles corresponding to 50 billion Monte Carlo moves. It is apparent that there is very little variation about the mean value.

A limitation[29] of the conventional Monte Carlo algorithm in the vicinity of a phase transition is that it is nonergodic, i.e., some regions of phase space become totally inaccessible. A consequence of nonergodic behavior for the hard sphere system is that the isotropic fluid curve has a metastable extension (phenomenon I) at packing fractions above that of the freezing point. An "overheated" region can also be expected to extend the solid curve (phenomenon II) to packing fractions that are less than that of the melting point. Various cluster[22,30] Monte Carlo algorithms have been proposed which overcome this problem. However these algorithms are currently restricted[31] to two dimensions and as such they cannot be used for hard spheres. In contrast, molecular dynamics is free from this type of nonergodic problem.

In view of the above considerations, is the new phase (phenomenon III) simply an artificial consequence of nonergodic Monte Carlo sampling? To answer this question we have also performed molecular dynamics[32] simulations for the hard sphere system. If the molecular dynamics simulations are started from a conventional fcc lattice, only the isotropic and solid regions are observed without metastable regions. However, if molecular dynamics simulations are commenced from a Monte Carlo generated configuration on the metastable curve (phenomenon I), the new phase (phenomenon III) is observed. Figure 9 shows that applying molecular dynamics to the metastable configuration results in a rapid drop in the compressibility factor. The new configuration obtained from molecular dynamics has the same character as reported from Monte Carlo calculations alone. The new values of the compressibility factor are consistent with the values obtained from Monte Carlo simulations of the new phase (phenomenon III). Figure 1 shows that there is reasonable qualitative agreement between the compressibility fac-

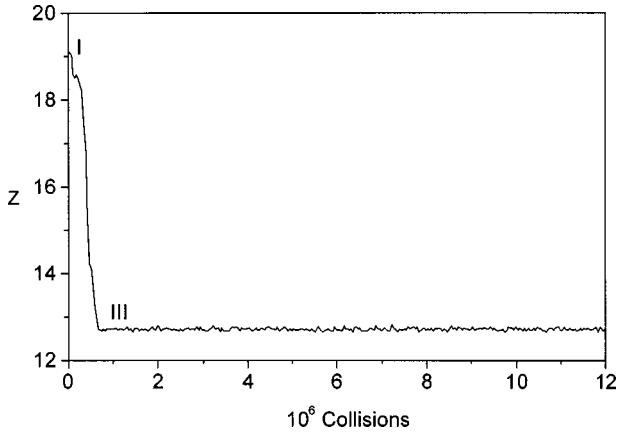


FIG. 9. Change in the compressibility factor resulting in the application of molecular dynamics to starting a configuration on the metastable curve (phenomenon I) at $\eta=0.550$. The rapid drop in the compressibility factor marks the formation of a new phase (phenomenon III).

tors for the new phase obtained from either Monte Carlo or molecular dynamics simulation. The data presented in Fig. 8(b) indicate that the new phase obtained from molecular dynamics is persistent beyond the equilibration period. The fact that phenomenon III can be obtained from molecular dynamics as well as Monte Carlo simulations provide strong evidence that the new phase is real.

## IV. CONCLUSIONS

A new phase for hard spheres was observed with a structure that does not conform to the conventional isotropic fluid, metastable, or solid phases. The new phase is stable. This result significantly alters our previous understanding of the behavior of hard spheres.

## ACKNOWLEDGMENT

The Australian Partnership for Advanced Computing (APAC) provided a generous allocation of computing time.

[1] N. A. Metropolis, A. W. Rosenbluth, M. N. Rosenbluth, A. H. Teller, and E. Teller, J. Chem. Phys. **21**, 1087 (1953).
[2] W. W. Wood and J. D. Jacobson, J. Chem. Phys. **27**, 1207 (1957).
[3] B. J. Alder and T. E. Wainwright, J. Chem. Phys. **27**, 1208 (1957).
[4] B. J. Alder and T. E. Wainwright, J. Chem. Phys. **33**, 1439 (1960).
[5] G. Hoover and F. H. Ree, J. Chem. Phys. **49**, 3609 (1968).
[6] J. A. Barker and D. Henderson, Mol. Phys. **21**, 187 (1971).
[7] J. J. Erpenbeck and W. W. Wood, J. Stat. Phys. **35**, 321 (1984).
[8] R. J. Speedy, Mol. Phys. **95**, 169 (1998).
[9] M. Robles, M. López de Haro, A. Santos, and S. B. Yuste, J. Chem. Phys. **108**, 1290 (1998).
[10] S. R. Williams, I. K. Snook, and W. van Megen, Phys. Rev. E **64**, 021506 (2001).
[11] P. G. Debenedetti and F. H. Stillinger, Nature (London) **410**, 259 (2001).
[12] R. J. Speedy, J. Phys. Chem. B **103**, 4060 (1999).
[13] F. H. Stillinger, Science **267**, 1935 (1995).
[14] C. A. Angell, Science **267**, 1924 (1995).
[15] R. J. Sadus, *Molecular Simulation of Fluids: Theory, Algorithms and Object-Orientation* (Elsevier, Amsterdam, 1999).
[16] M. D. Rintoul and S. Torquato, Phys. Rev. E **58**, 532 (1998).
[17] P. G. Debenedetti, *Metastable Liquids* (Princeton University Press, Princeton, New Jersey, 1996).
[18] J. W. Perram and M. S. Wertheim, Chem. Phys. Lett. **105**, 277 (1984).
[19] J. W. Perram and M. S. Wertheim, J. Comput. Phys. **58**, 409 (1985).
[20] J. G. Berryman, Phys. Rev. A **27**, 1053 (1983).
[21] T. Gruhn and P. A. Monson, Phys. Rev. E **64**, 061703 (2001).
[22] L. Stanten and W. Krauth, Nature (London) **405**, 550 (2000).
[23] J.-P. Hansen and I. R. McDonald, *Theory of Simple Liquids*, 2nd ed. (Academic, London, 1986).
[24] W. Kob and H. C. Andersen, Phys. Rev. E **52**, 4134 (1995).
[25] G. Foffi, W. Götze, F. Sciortino, P. Tartaglia, and Th. Voigtmann, Phys. Rev. Lett. **91**, 085701 (2003).
[26] S. C. McGrother, D. C. Williamson, and G. J. Jackson, Chem. Phys. **104**, 6755 (1996).
[27] T. M. Truskett, S. Torquato, and P. G. Debenedetti, Phys. Rev. E **62**, 993 (2000).
[28] P. R. ten Wolde, M. J. Ruiz-Montero, and D. Frenkel, J. Chem. Phys. **104**, 9932 (1996).
[29] J. Valleau in *Monte Carlo Methods in Chemical Physics*, *Advances in Chemical Physics*, edited by D. M. Ferguson, J. I. Siepmann, and D. G. Truhlar (Wiley, New York, 1999), Vol. 105.
[30] C. Dress and W. Krauth, J. Phys. A **28**, L587 (1995).
[31] W. Krauth (personal communication).
[32] M. P. Allen and D. J. Tildesley, *Computer Simulation of Liquids* (Clarendon, Oxford, 1987).